

Second enhancement in surface-enhanced resonance Raman scattering revealed by an analysis of anti-Stokes and Stokes Raman spectra

Tamitake Itoh,^{1,*} Kenichi Yoshida,² Vasudevanpillai Biju,¹ Yasuo Kikkawa,² Mitsuru Ishikawa,¹ and Yukihiro Ozaki²
¹*Nano-Bioanalysis Team, Health Technology Research Center, National Institute of Advanced Industrial Science and Technology (AIST), Takamatsu, Kagawa 761-0395, Japan*

²*Department of Chemistry, School of Science and Technology, Kwansai Gakuin University, Sanda, Hyogo 669-1337, Japan*

(Received 13 June 2007; published 6 August 2007)

Evidence of “twofold” electromagnetic (EM) enhancement in surface-enhanced resonance Raman scattering (SERRS) that exhibits a SERRS enhancement factor of up to 10^{14} has been analyzed by comparing SERRS spectra and plasmon resonance Rayleigh scattering spectra. We identified that SERRS spectral variations are induced by selective enhancement of SERRS bands whose maxima are close to plasmon resonance maxima. The correlation between the selective enhancement of SERRS and the plasmon energy demonstrated that the variations in SERRS spectra are induced by second EM enhancement in SERRS as a result of coupling between scattering photons and plasmons.

DOI: [10.1103/PhysRevB.76.085405](https://doi.org/10.1103/PhysRevB.76.085405)

PACS number(s): 78.30.-j, 33.20.Fb, 78.67.Bf, 82.65.+r

I. INTRODUCTION

Surface-enhanced resonance Raman scattering (SERRS) has recently attracted great interest in analytical science due to enormous enhancement factors that have increased the detection limits of a wide variety of molecules to the single molecule level.¹⁻⁵ The SERRS-electromagnetic (EM) model describes single-molecule SERRS sensitivity at interparticle junctions and at sharp edges in Ag and Au nanoaggregates based on the fourth power of a local EM-field enhancement factor M .^{3,6-11} The realization of SERRS enhancement factors $|M|^4$ of up to 10^{14} has made single-molecule sensitivity realistic. In other words, twofold EM enhancement processes are important for verifying SERRS enhancement factors that enable single molecules to be detected; in these processes the first enhancement is due to coupling between incident photons and plasmons and the second enhancement is due to coupling between SERRS photons and plasmons.¹²⁻¹⁶ The relationship between plasmon resonance, the SERRS intensity, and Ag-nanoparticle microstructures was comprehensively studied to verify EM enhancement in SERRS.¹⁷⁻²¹ However, the first and second enhancements were not treated independently in these investigations and thus they were not able to provide conclusive evidence for twofold EM enhancements.

Large variations in SERRS spectra have frequently been observed between different nanoaggregates.¹⁻⁵ We consider that these variations in SERRS spectra are the key for elucidating twofold EM enhancement processes. According to the context of the second enhancement in SERRS,¹²⁻¹⁶ the variations in SERRS spectral shapes can be explained in terms of fluctuating plasmon resonance frequencies. This is because the coupling efficiency between SERRS photons and plasmons depends greatly on the plasmon resonance frequencies. Thus careful comparison between SERRS spectral shapes and plasmon resonance band shapes of single nanoaggregates would provide convincing evidence of the twofold EM enhancement mechanism.

In this current study, we identified that variations in SERRS spectra are present in both the Stokes and anti-

Stokes regions. By comparing Stokes and anti-Stokes SERRS spectra with plasmon resonance Rayleigh scattering spectra, we ascertained that the variations were from selective enhancement of SERRS bands whose maxima were close to the plasmon resonance maxima. In other words, we found that the origin of the variations is the second enhancement due to coupling between SERRS photons and plasmons. Furthermore, we reproduced the variations in SERRS spectra by taking the product of an ensemble-averaged SERRS spectrum with the plasmon resonance band of a single nanoaggregate. Finally, we discuss the discrepancy between the experimental and calculated SERRS spectra in terms of (i) the difference between spectra of EM field intensity of Ag nanoaggregates and those of localized SERRS active sites on Ag nanoaggregates and (ii) the molecular pre-resonance effect on SERRS spectra.

II. EXPERIMENT

An Ag nanoparticle colloidal solution was prepared following the method of Lee and Meisel.²² An aqueous solution containing rhodamine 123 (R123, 6.5×10^{-8} M) and NaCl (10 mM) was mixed with an Ag nanoparticle colloidal solution (7.2×10^{-11} M) and incubated for 30 min at room temperature (20 °C). The concentration of R123 was greater than that employed in standard single-molecule SERRS experiments ($\sim 10^{-11}$ M) in order to avoid spectral fluctuation and blinking due to molecular diffusion on the silver surfaces; such spectral properties obscure the expected relationship between plasmon resonance and SERRS spectra. Sample preparation methods and the spectroscopic setup are described elsewhere.¹⁸ Briefly, a 100-W halogen lamp was used as a white-light source to measure plasmon resonance Rayleigh scattering and a dark-field condenser lens was used to focus the laser illumination onto the Ag nanoaggregates. A Kr⁺ laser was used for SERRS excitation at 568 and 647 nm. The integration time was 5 s for each spectrum. The intensities of the plasmon resonance Rayleigh scattering spectra were calibrated using the white-light source.

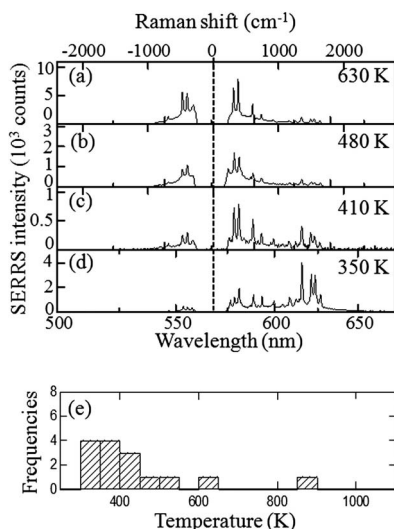


FIG. 1. (a)–(d) Anti-Stokes and Stokes SERS spectra from four representative Ag nanoaggregates excited at 568 nm. The vertical dashed line indicates the excitation-laser wavelength. (e) A histogram of estimated molecular temperatures for individual Ag nanoaggregates.

III. RESULTS AND DISCUSSION

Variations in Stokes and anti-Stokes SERS spectra have been investigated as a function of molecular temperature²³ and stimulated Raman processes^{21,24} rather than second enhancement in SERS. We reinvestigated the effect of the temperature of R123 molecules on Ag nanoaggregates by using the intensity ratios of anti-Stokes to Stokes vibrational bands.²⁵ Figures 1(a)–1(d) show SERS spectra of four representative single Ag nanoaggregates. We estimated the molecular temperatures by assuming a Boltzmann distribution. The estimated molecular temperatures were 630, 480, 410, and 340 K for the SERS bands in Figs. 1(a)–1(d), respectively. The estimated molecular temperatures for single nanoaggregates are summarized in Fig. 1(e). Interestingly, the molecular temperatures exceeded the decomposition temperature of R123 (540 K) in several cases. Thus these temperatures may not be “real” temperatures, that is, the origin of the variations in the anti-Stokes and Stokes SERS intensities is not directly related to the temperatures of SERS-active molecules. We also examined the relationship between spectral variations and variations in the stimulated Raman scattering. In a previous report, the exponential dependence of anti-Stokes SERS intensities on the excitation laser power was determined for excitation intensities between 10 and 10^4 W/cm².²⁴ That investigation discussed anti-Stokes SERS in terms of stimulated Raman process. We therefore assume that the variations in SERS spectra were induced by variations in the stimulated Raman process. We investigated the dependence of the anti-Stokes and Stokes SERS intensities on the excitation-laser power for low-power excitations (0.3–6.5 W/cm²). Both the anti-Stokes and Stokes intensities increased linearly with an increase in the laser power, as shown in Fig. 2(a). This linearity demonstrates that the stimulated Raman process is inadequate for explaining

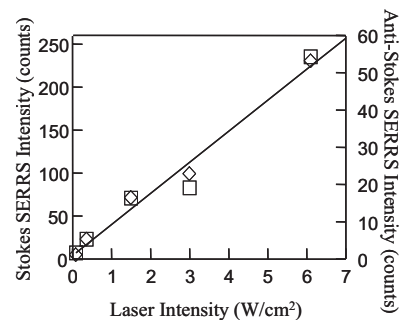


FIG. 2. Laser power dependence of intensities of anti-Stokes SERS maxima (\square) and Stokes SERS maxima (\sqcap) for SERS bands around -420 cm⁻¹ and $+420$ cm⁻¹.

the variations in SERS spectra under low excitation powers when compared to the results in Ref. 24.

Thus we have excluded molecular temperature and stimulated Raman processes as origins of the variations in the SERS spectra obtained in this current study. We examined the possibility of the variations in anti-Stokes and Stokes SERS spectra being caused by the second enhancement in the SERS-EM model, that is, coupling between SERS photons and plasmons.^{3,6–9} The SERS-EM model gives a simple expression for the total SERS enhancement by assuming that it is the product of the enhancements of the incident and scattered light produced by plasmon resonance.^{1,3,7,8} Thus the total enhancement factor M_{total} of SERS is given by

$$M_{total} = \left| \frac{E^{Loc}(\lambda_L)}{E^I(\lambda_L)} \right|^2 \times \left| \frac{E^{Loc}(\lambda_L \pm \lambda_R)}{E^I(\lambda_L \pm \lambda_R)} \right|^2 = M_1(\lambda_L) \times M_2(\lambda_L \pm \lambda_R), \quad (1)$$

where E^I and E^{Loc} are the amplitudes of the incident and local electronic fields, respectively, λ_L is the excitation wavelength, $+\lambda_R$ and $-\lambda_R$ are the wavelengths of the anti-Stokes and Stokes shifted Raman scattering, respectively, and M_1 and M_2 are the first and second enhancement factors, respectively. The spectrum of $M_2(\lambda)$ is expected to be similar to that of plasmon resonance Rayleigh scattering, since the second enhancement was produced by scattering of Raman light through plasmon resonance.^{6,10,11} Thus the dependence of SERS spectra on plasmon-resonance maxima is a key observation for identifying the origin of the variations in SERS spectra as fluctuations in the second enhancement. However, the EM fields on larger Ag nanoparticle aggregates are complicated due to the dipole and multipoles overlapping.²⁶ Thus characterization of the dependence of SERS spectra on plasmon-resonance maxima will be difficult. This difficulty was overcome by selecting Ag nanoaggregates with dipole plasmons that satisfy the following two criteria: the polarization dependence of a plasmon resonance maximum follows a cosine-squared law, and the SERS maxima and plasmon resonance maxima have the same polarization dependence. As a consequence of applying these two criteria, we were able to exclusively identify dipole plasmons that were coupled with SERS.^{18–20}

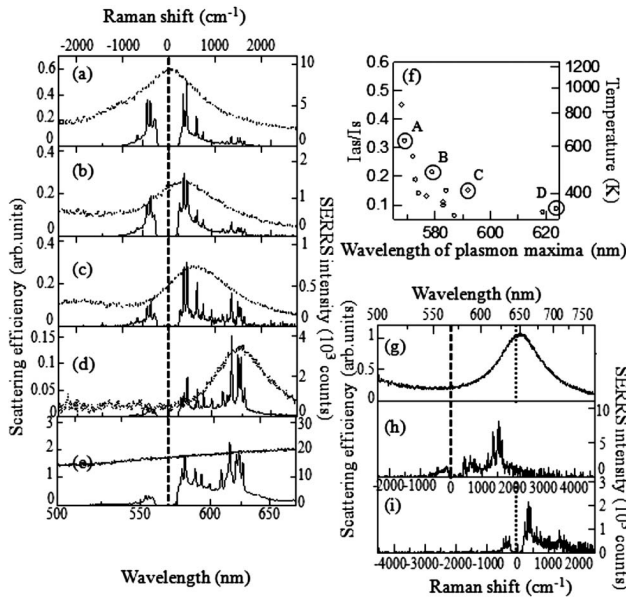


FIG. 3. (a)–(d) Anti-Stokes and Stokes SERS spectra (solid lines) and plasmon resonance Rayleigh scattering spectra (dotted lines) from four representative nanoaggregates, and (e) those from one large aggregate. The vertical dashed line indicates the excitation-laser wavelength. Plasmon-resonance Rayleigh-scattering maxima in (a)–(d) were observed at 568, 577, 588, and 623 nm. (f) Plasmon-resonance maxima dependence of anti-Stokes to Stokes intensity ratios. Doubly circled points indicated by A–D correspond to the data in (a)–(d), respectively. (g) Plasmon-resonance Rayleigh scattering spectra, (h) SERS spectra excited at 568 nm, and (i) SERS spectra excited at 647 nm. All spectra in (g)–(i) were obtained from the same Ag nanoaggregate.

Figures 3(a)–3(d) show Rayleigh scattering spectra and SERS spectra from five Ag nanoaggregates that were selected based on the above two criteria. We observed that the SERS bands close to the plasmon resonance maxima were selectively enhanced. For example, the intensities of the anti-Stokes bands close to the plasmon resonance maximum in Fig. 3(a) were larger than those of the anti-Stokes bands shown in Figs. 3(b)–3(d). Figure 3(b) shows that the intensities of the Stokes bands in the vicinity of 400 cm^{-1} were much larger than those around 1500 cm^{-1} . On the other hand, Fig. 3(d) shows that the intensities of Stokes bands around 1500 cm^{-1} are larger than those around 400 cm^{-1} . Interestingly, the enhanced bands were close to the plasmon resonance maximum in both cases. This selective enhancement shows a correlation between the spectra of the SERS enhancement factor and plasmon-resonance maxima. Thus this selective enhancement provided a possibility of experimentally verifying the second enhancement in SERS. It should be noted that the larger SERS-active Ag aggregates having sizes of several micrometers did not exhibit aggregate-to-aggregate variations in their SERS and Rayleigh scattering spectra, as shown in Fig. 3(e). This absence of variations is due to inhomogeneous broadening of the plasmon resonance bands and averaging of the SERS spectra. Variations in the SERS and Rayleigh scattering spectra were observed only in the case of smaller Ag aggregates that

were several tens to hundreds of nanometers in size.

Figure 3(f) summarizes the plasmon resonance maxima dependence of the anti-Stokes to Stokes intensity ratios of SERS maxima at 553 nm ($+634\text{ cm}^{-1}$) and 580 nm (-634 cm^{-1}). According to Eq. (1) this ratio is given by $M_1(\lambda_L)M_2(\lambda_L-\lambda_R)/M_1(\lambda_L)M_2(\lambda_L+\lambda_R)$; thus the first enhancement factor $M_1(\lambda_L)$ cancels. Experimentally, we identified a reduction in the ratios with increasing redshifts of the plasmon resonance maxima. This reduction in the ratio, $M_1(\lambda_L-\lambda_R)/M_2(\lambda_L+\lambda_R)$, is attributed to a decrease in the coupling efficiency of anti-Stokes photons and plasmons due to separation of the plasmon resonance maxima from anti-Stokes bands; this supports the conjecture that the origin of variations in anti-Stokes and Stokes SERS spectra is fluctuations in the second enhancement factor of the SERS-EM model.

We examined the excitation-wavelength dependence of SERS spectra for single Ag nanoaggregates and confirmed the plasmon-resonance maxima dependence of SERS spectra. Figure 3(g) shows the plasmon resonance maximum at 650 nm of a typical Ag nanoaggregate. SERS spectra of the aggregate when it was excited at 568 and 647 nm are shown in Figs. 3(h) and 3(i), respectively. The intensities of SERS bands around 630 nm in Fig. 3(h), and 660 nm in Fig. 3(i) were larger than those around 580 and 710 nm. From these observations it is apparent that the SERS bands close to the plasmon resonance maxima were selectively enhanced and that this effect is excitation-wavelength dependent. This excitation-wavelength dependence demonstrates that the intensity of SERS spectra depends on the plasmon-resonance maxima through the second enhancement process in the SERS-EM model.

SERS spectra of larger Ag aggregates [see Fig. 3(e)] did not show aggregate-to-aggregate variations. This lack of variations indicates that the observed SERS spectra were averaged spectra for a large number of Ag nanoaggregates. In light of the second enhancement, this lack of variations shows that the plasmon resonance bands that contribute to the second enhancement in SERS are uniformly overlapped. Indeed, Rayleigh scattering spectra of such large Ag aggregates consisted of broad peaks that extended over the entire visible spectrum, as shown in Fig. 3(e). Therefore we assumed that spectra of the second enhancement factors of such large aggregates are also broad. Based on this consideration we calculated the SERS spectrum of a single Ag nanoaggregate, $I_S(\lambda)$, by taking the product of a SERS spectrum of a large aggregate, $I_S(\lambda)$, with a plasmon resonance Rayleigh scattering spectrum of a single Ag nanoaggregate, $I_P(\lambda)$, that is, $I_S(\lambda) = I_S(\lambda) \times I_P(\lambda)$. In this calculation, we assume that the spectra of the second enhancement factors of individual Ag nanoaggregates were proportional to the plasmon resonance spectra of individual Ag nanoaggregates, that is, $M_2(\lambda) \propto I_P(\lambda)$. Background luminescence spectra from SERS spectra were always subtracted before performing these calculations so as to simply investigate Eq. (1).

Figures 4(a)–4(d) show the calculated and the measured SERS spectra; plasmon resonance Rayleigh scattering spectra of different isolated single Ag nanoaggregates are

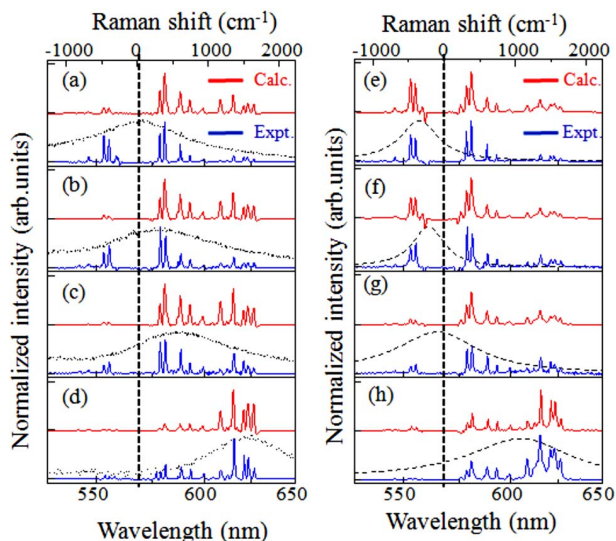


FIG. 4. (Color online) (a)–(d) Experimental SERRS spectra (blue lines) and calculated SERRS spectra [red lines, multiplication SERRS spectra in Fig. 3(a) by each plasmon resonance band] and plasmon resonance Rayleigh scattering spectra (dotted lines). (e)–(h) Experimental (blue lines) and calculated SERRS spectra [red lines, multiplication SERRS spectra in Fig. 3(a) by each Lorentzian curve] and the four Lorentzian resonance spectra (dotted lines). The experimental and the calculated SERRS spectra in (a)–(h) were normalized at their spectral maxima. The calculated SERRS spectra in (a)–(h) were offset vertically to distinguish experimental SERRS spectra. Background luminescence spectra were subtracted from SERRS spectra in Fig. 3 before obtaining the products.

included in each figure. There was reasonable agreement between the calculated SERRS spectra and the experimentally measured SERRS spectra in the Stokes region but poor agreement between them in the anti-Stokes region. This poor agreement is probably due to the deviation of the $M_2(\lambda)$ spectra from the experimental plasmon resonance Rayleigh scattering spectra. We consider that the deviation is acceptable because $M_2(\lambda)$ is proportional to a spectrum of EM field intensity at a SERRS active site localized on single Ag nanoaggregate but a plasmon resonance Rayleigh scattering spectrum is proportional to a spectrum of EM field intensity of whole single Ag nanoaggregate. Indeed, it is theoretically shown that both spectra of EM field intensity are a little deviated from each other.²⁷ We changed the spectral shapes of $M_2(\lambda)$ from experimental plasmon resonance Rayleigh scattering spectra to Lorentzian curves $I_L(\lambda)$ to improve the agreement between the calculated and measured anti-Stokes bands, and then recalculated $I_{SS}(\lambda) = I_{Sf}(\lambda) \times I_L(\lambda)$.²⁸ This calculation is not only for improvement of agreement but also for examination of spectra of EM field intensity at SERRS active sites localized on Ag nanoaggregates. We used Lorentzian curves for the recalculation because selected isolated single Ag nanoaggregates have dipolar plasmons coupled with SERRS.²⁰ Since the selected Ag nanoaggregate is expected to be enough smaller than the excitation wavelength, its scattering cross-section spectrum $C_{sca}(\lambda) [\propto I_P(\lambda)]$ can be approximately treated by dipole radiation using quasi-Rayleigh approximation.^{29,30} That is, $C_{sca}(\lambda) = (k^4/6\pi)\alpha(\lambda)^2$,

where k is the wave number, $\alpha(\lambda) = V\{L - \varepsilon_m / [\varepsilon(\lambda) - \varepsilon_m] - (i4\pi\varepsilon_m^{3/2}V)/(3\lambda^3)\}$ is the polarizability, L is the depolarization factor, $\varepsilon(\lambda) [\equiv \varepsilon_1(\lambda) - i\varepsilon_2(\lambda)]$ is the complex relative permittivity of the Ag nanoaggregate, ε_m is the relative permittivity of the surrounding medium, V is the volume, and $(i4\pi\varepsilon_m^{3/2}V)/(3\lambda^3)$ is radiation damping.²⁶ Plasmon resonance peak wavelengths in the present experiments are in the region 560–630 nm. In this wavelength region, $\varepsilon_1(\lambda)$ is much larger than $\varepsilon_2(\lambda)$,³¹ and consequently dephasing of the dipole oscillation of the plasmon is dominated by the radiation damping; thus the spectrum of $C_{sca}(\lambda)$ can be represented by a simple Lorentzian function. Thus we considered that Lorentzian functions are suitable for fitting of the homogeneous line shapes of plasmon resonance Rayleigh scattering spectra. Figures 4(e)–4(h) show comparisons of the recalculated and measured SERRS spectra. The Lorentzian maxima in Figs. 4(e)–4(h) (557, 561, 566, 606 nm) were always blueshifted from the experimental plasmon resonance maxima (568, 577, 588, 623 nm) by ~ 3 –20 nm. We expect that the blueshifts are results of difference between spectra of EM field intensity of whole single Ag nanoaggregates and those of localized sites on Ag nanoaggregates.²⁷ However, from a study of resonance Raman scattering spectra, there is another possibility for the reason of the difference that the blueshifts were produced by preresonance Raman enhancement due to molecular electronic resonance.³² In the case of the preresonance Raman excitation, anti-Stokes bands have larger resonance enhancements than Stokes bands because the wavelength of anti-Stokes light is closer to wavelength of the laser light than the wavelength of Stokes light.³² Accordingly, the anti-Stokes band intensity becomes larger than that without the preresonance Raman enhancement. We thus add another possibility that the deviation of $M_2(\lambda)$ from plasmon resonance Rayleigh scattering spectra occurred because preresonance Raman enhancement for anti-Stokes SERRS bands was larger than that for Stokes SERRS bands.

IV. SUMMARY

In the current study, we investigated the origin of nanoaggregate-to-nanoaggregate variation in anti-Stokes and Stokes SERRS spectra by comparing SERRS spectra and plasmon resonance Rayleigh scattering spectra from single Ag nanoaggregates. By investigating the selective enhancement of SERRS bands whose maxima were close to the plasmon resonance maxima, we found that the second enhancement in the SERRS process induced variations in the SERRS spectra. Furthermore, the spectra of the second enhancement factors were blueshifted from the plasmon resonance Rayleigh scattering spectra by 3–20 nm through the difference between spectra of EM field intensity of Ag nanoaggregates and those of localized sites on Ag nanoaggregates or through preresonance Raman enhancement of SERRS bands.

ACKNOWLEDGMENTS

This work was supported by an ‘‘Open Research Center’’ project for private universities with a matching fund subsidy from MEXT.

*tamitake-itou@aist.go.jp

- ¹K. Kneipp, Y. Wang, H. Kneipp, L. T. Perelman, I. Itzkan, R. R. Dasari, and M. S. Feld, *Phys. Rev. Lett.* **78**, 1667 (1997).
- ²S. M. Nie and S. R. Emory, *Science* **275**, 1102 (1997).
- ³H. Xu, E. J. Bjerneld, M. Käll, and L. Borjesson, *Phys. Rev. Lett.* **83**, 4357 (1999).
- ⁴A. M. Michaels, M. Nirmal, and L. E. Brus, *J. Am. Chem. Soc.* **121**, 9932 (1999).
- ⁵S. Habuchi, M. Cotlet, R. Gronheid, G. Dirix, J. Michiels, J. Vanderleyden, F. D. Schryver, and J. Hofkens, *J. Am. Chem. Soc.* **125**, 8446 (2003).
- ⁶M. Inoue and K. Ohtaka, *J. Phys. Soc. Jpn.* **52**, 3853 (1983).
- ⁷M. Moskovits, *Rev. Mod. Phys.* **57**, 783 (1985).
- ⁸F. J. García-Vidal and J. B. Pendry, *Phys. Rev. Lett.* **77**, 1163 (1996).
- ⁹E. Hao and G. C. Schatz, *J. Chem. Phys.* **120**, 357 (2004).
- ¹⁰H. Xu, X. H. Wang, M. P. Persson, H. Q. Xu, M. Käll, and P. Johansson, *Phys. Rev. Lett.* **93**, 243002 (2004).
- ¹¹B. J. Pettinger, *J. Chem. Phys.* **85**, 7442 (1986).
- ¹²M. Kerker, D. S. Wang, and H. Chew, *Appl. Opt.* **19**, 4159 (1980).
- ¹³J. Gersten and A. Nitzan, *J. Chem. Phys.* **73**, 3023 (1980).
- ¹⁴D. A. Weitz, S. Garoff, J. I. Gersten, and A. Nitzan, *J. Chem. Phys.* **78**, 5324 (1983).
- ¹⁵M. Inoue and K. Ohtaka, *Phys. Rev. B* **26**, 3487 (1982).
- ¹⁶A. D. McFarland, M. A. Young, J. A. Dieringer, and R. P. VanDuyne, *J. Phys. Chem. B* **109**, 11279 (2005).
- ¹⁷I. Khan, D. Cunningham, D. Graham, D. W. McComb, and W. E. Smith, *J. Phys. Chem. B* **109**, 3454 (2005).
- ¹⁸T. Itoh, K. Hashimoto, and Y. Ozaki, *Appl. Phys. Lett.* **83**, 2274 (2003).
- ¹⁹T. Itoh, K. Hashimoto, A. Ikehata, and Y. Ozaki, *Chem. Phys. Lett.* **389**, 225 (2004).
- ²⁰T. Itoh, V. Biju, M. Ishikawa, Y. Kikkawa, K. Hashimoto, A. Ikehata, and Y. Ozaki, *J. Chem. Phys.* **124**, 134708 (2006).
- ²¹R. C. Maher *et al.*, *J. Chem. Phys.* **120**, 11746 (2004).
- ²²P. C. Lee and D. J. Meisel, *J. Phys. Chem.* **86**, 3391 (1982).
- ²³Y. Maruyama, M. Ishikawa, and M. Futamata, *J. Phys. Chem. B* **108**, 673 (2004).
- ²⁴K. Kneipp, Y. Wang, H. Kneipp, I. Itzkan, R. R. Dasari, and M. S. Feld, *Phys. Rev. Lett.* **76**, 2444 (1996).
- ²⁵J. Chowdhury, P. Pal, M. Ghosh, and T. N. Misra, *J. Colloid Interface Sci.* **235**, 317 (2001). We used the anti-Stokes and Stokes SERRS bands of R123 which arise from the torsional mode of the xanthene ring at 553 and 580 nm ($\pm 634 \text{ cm}^{-1}$) for temperature estimation.
- ²⁶U. Kreibig and M. Vollmer, *Optical Properties of Metal Clusters*, Springer Series in Materials Science Vol. 25 (Springer, Berlin, 1995).
- ²⁷B. J. Messinger, K. U. von Raben, R. K. Chang, and P. W. Barber, *Phys. Rev. B* **24**, 649 (1981).
- ²⁸We used the following procedure to determine the value of the peak wavelength λ_{pk} and the full width at half maximum ($\Delta\lambda$) of a Lorentzian-fitted spectrum $I_L(\lambda)$. (i) λ_{pk} and $\Delta\lambda$ were set to be the same as those of a measured plasmon resonance Rayleigh scattering spectrum $I_P(\lambda)$. (ii) $I_{SI}(\lambda) \times I_L(\lambda)$ was calculated, where $I_{SI}(\lambda)$ is the SERRS spectrum of a large Ag aggregate. (iii) λ_{pk} was varied to better reproduce the Stokes and anti-Stokes bands of $I_{SS}(\lambda)$ from 550 to 580 nm (in the spectral vicinity of the Rayleigh line) by $I_{SI}(\lambda) \times I_L(\lambda)$, where $I_{SS}(\lambda)$ is the SERRS spectrum of a small Ag nanoaggregate. (iv) $\Delta\lambda$ was varied to better reproduce the Stokes and anti-Stokes bands of $I_{SS}(\lambda)$ by $I_{SI}(\lambda) \times I_L(\lambda)$ from 500 to 650 nm. (v) Steps (iii) and (iv) were repeated until $I_{SI}(\lambda) \times I_L(\lambda)$ was close to $I_{SS}(\lambda)$.
- ²⁹T. Klar, M. Perner, S. Grosse, G. von Plessen, W. Spirkl, and J. Feldmann, *Phys. Rev. Lett.* **80**, 4249 (1998).
- ³⁰H. Kuwata, H. Tamaru, K. Esumi, and K. Miyano, *Appl. Phys. Lett.* **4625**, 83 (2003).
- ³¹P. B. Johnson and R. W. Christy, *Phys. Rev. B* **6**, 4370 (1972).
- ³²H. Okamoto, T. Nakabayashi, and M. Tasumi, *J. Phys. Chem. B* **101**, 3488 (1997).